A Model for Hybrid Dynamic Beam Movement with Specific Application to Wind Energy Units

Ramakanta Patra

Thesis submitted to the Faculty of the Virginia Polytechnic Institute and State University in partial fulfillment of the requirements for the

degree of

Master of Science

in

Mathematics

David L. Russell, Chair

Robert L. Wheeler

Jong Uhn Kim

August 8, 2011

Blacksburg, Virginia

Keywords: Hybrid Dynamic Systems, Optimal Control.

A Model for Hybrid Dynamic Beam Movement with Specific Application to Wind Energy Units

Ramakanta Patra

Abstract

The aim of this thesis is to present a structural model for a wind turbine and its supporting pylon, to analyze and simulate attendant vibration phenomena and to suggest and simulate an appropriate control procedure. A wind turbine can be described as an elastic system consisting of distributed parameter, beam and rod type, elements coupled to a rotating lumped mass generator/turbine component at one end. We allow for both lateral and torsional movements of the beam. Solution methods for related vibration and control problems are suggested and analyzed. Results of computations for sample problems are presented. Applications of control of structural vibrations in wind energy units using proof mass type actuators as part of the tip mass are also analyzed.

Dedication

To my father, Shree Shreemanta Kishore Patra, who is also my first teacher in mathematics.

Acknowledgements

This research would have been impossible without the help of two very important people, my adviser Professor David L. Russell and my wife Shreemati Anjali Panai Patra. I would like to take this opportunity to thank Professor Russell for the enormous time he put into giving me lessons on different topics which were essential in developing this thesis. His encouragement, support and patience during every step of this thesis and his putting up with my untimely needs has been outstanding. Thanks are also due to Professor Russell for providing me with a quiet study space where I carried out most of my research. I also want to take this opportunity to thank my wife, Anjali, for working relentless hours to support my education and not letting me into financial and emotional distress. I cannot imagine what life would have been without her support during the time this piece of research was carried out. Thanks are also due to Professor Robert Wheeler who served as a committee member and came up with numerous suggestions on how to improve the thesis and proofread my paper in a very careful manner. I also want to thank Professor Jong Uhn Kim for serving on my thesis committee. Finally, I want to thank The Almighty for being with me all through this tenuous journey.

Table of Contents

List of Figures

1 Introduction and Mathematical Formulation

1.1 Background

The objective of this research is to study a controlled wind turbine as a distributed parameter system coupled to a tip mass, part of which is rotating, attached to the free end of the structure. Non-technical background material may be found, e.g., in [10]. The beam is fixed at the ground end, bends in two dimensions and, in addition, undergoes torsional motion. The "head" element of the structure, which houses a generating unit, etc., is modeled as a mass attached to the free end of the beam which includes the wind fan as a rotating component. At different levels of realism the rotating mass may be interpreted as rigid unit, or the blades may be individually modeled within, e.g., a *narrow beam* aeroelastic framework. The first approach is pursued in this work.

Control action to counteract variable wind strength with attendant variable fan rotation is studied and controlled model studies are undertaken via extensive computer simulation.

There is a considerable body of scientific literature pertinent to our study. The mathematical history relevant to the present project goes back to the early studies of elastic beam vibrations in the 1960's and 1970's [13], [12], [9]. Literally hundreds of papers have appeared since , covering numerous aspects of the subject. In the 1980's NASA's *Spacecraft Control Laboratory Experiment*, acronym SCOLE, which concerned an antenna connected to the space shuttle by a flexible beam structure led to many contributions in the area of elastic beams with a connected *tip mass*.

1.2 A Hybrid Structure; Energy Expressions

Structurally, a wind energy unit can be considered as a distributed system consisting of a beam with torsion in R^3. We consider this to be a right handed system with the logitudinal, x, axis of the beam extending in the vertical direction with the beam clamped rigidly to the ground at $x = 0$. At the free end, $x = L$, a lumped parameter system representing a generator head and wind turbine, is rigidly attached to the beam, which represents the supporting pylon for the assembly. The y axis is transverse to the axis of the fan when at rest and the z axis measures the longitudinal direction of the fan axis and the angle θ is measured in the standard positive direction in the y, z plane. We consider the motion of the beam with the projection of the beam displacement onto the x, y plane represented by a smooth function $y(x,t)$ and the corresponding projection on to the x, z plane by $z(x,t)$. We will denote the torsional displacement in the y, z positive direction about the x-axis by $\theta(x,t)$.

We assume a prismatic Euler-Bernoulli beam model [1], [7] which is symmetric with respect to

the y and z axes and we denote it's stiffness coefficients by k_y, k_z, k_θ. Then the potential energy integrals coming from the lateral movements of the beam are

$$\frac{k_y}{2}\int_0^L \left(\frac{\partial^2 y}{\partial x^2}\right)^2 dx, \quad \frac{k_z}{2}\int_0^L \left(\frac{\partial^2 z}{\partial x^2}\right)^2 dx, \tag{1.1}$$

and the potential energy coming from the angular rotation about the x axis is

$$\frac{k_\theta}{2}\int_0^L \left(\frac{\partial^2 \theta}{\partial x^2}\right)^2 dx, \tag{1.2}$$

[5], [15] where

$$y = y(x,t), \quad z = z(x,t)$$

and $\theta = \theta(x,t)$. The sum of these three expressions is the total beam elastic potential energy which we denote by V_B.

Assuming the beam has mass density M_B per unit length and the moment of inertia per unit length I_B about the x axis, the kinetic energy integrals are

$$\frac{M_B}{2}\int_0^L \left(\frac{\partial^2 y}{\partial x^2}\right)^2 dx, \ \frac{M_B}{2}\int_0^L \left(\frac{\partial^2 z}{\partial x^2}\right)^2 dx, \ \frac{I_B}{2}\int_0^L \left(\frac{\partial^2 \theta}{\partial x^2}\right)^2 dx, \tag{1.3}$$

From now on, in order to simplify notation, we will frequently use $\dot{}$ to represent the t partial derivative and ' to represent the x partial derivative; viz.: $\dot{y}(x,t)$, $y'(x,t)$ etc..

In this research work we assume that the beam is rigidly fixed on the ground end and that the overall motion is sufficiently small in order that we may ignore any translational motion of the head in the x (vertical) direction. However, we will denote the translational motions in the y and z directions by Y(t) and Z(t) respectively. We will denote the rotational motions of the generator head in the x, y and x, z planes by $\Phi(t)$, $\Psi(t)$ and $\Theta(t)$ respectively.

Now we can formulate the kinetic energy of the generator head, not including the wind fan, as follows

$$T_H \equiv \frac{M_H}{2}\dot{Y}(t)^2 + \frac{M_H}{2}\dot{Z}(t)^2 + \frac{I_{xz}}{2}\dot{\Phi}(t)^2 + \frac{I_{xy}}{2}\dot{\Psi}(t)^2 + \frac{I_{yz}}{2}\dot{\Theta}(t)^2, \tag{1.4}$$

where M_H is the mass of the generator head,I_{xy} is the moment of inertia of the generator head about the z - axis, I_{yz} is the moment of intertia of the generator head about the x - axis and I_{xz} is the moment of inertia about the y - axis.

From the model's physical setting we can deduce the boundary conditions at the two ends of the beam. At the ground level where the beam is rigidly fixed, i.e., at $x = 0$, the boundary conditions of the beam are

$$y(0,t) = z(0,t) = \theta(0,t) = 0. \tag{1.5}$$

At the free end of the beam we assume that the generator head is rigidly attached to the beam at $x = L$. So the first order boundary conditions at $x = L$ are

$$y(L,t) = Y(t),\ z(L,t) = Z(t),\ \theta(L,t) = \Theta(t),\ \frac{\partial y}{\partial x}(L,t) = \Phi(t),\ \frac{\partial z}{\partial x}(L,t) = \Psi(t). \tag{1.6}$$

We assume the wind fan rotates about an axis passing through the center of mass of the generator head. The fan hub is located $D > 0$ units from the center of mass in the positive z direction when at rest.

In order to obtain the energy terms for the wind fan we introduce a new $\Xi = (\xi,\ \eta,\ \zeta)$ coordinate system, with the origin at the free end point of the moving beam, which translates and rotates with the free end point of the beam so that the free end point of the beam is always at rest with respect to that system of coordinates. We do some elementary computations as follows in order to obtain the change of coordinate relationship between the X, Y, Z and the ξ, η, ζ beam coordinates. For this we proceed as follows. The transformation matrix for θ rotation, which is the counter clock-wise rotation around the x axis, is

$$\begin{pmatrix} 1 & 0 & 0 \\ 0 & \cos(\Theta) & \cos(90+\Theta) \\ 0 & \cos(90-\Theta) & \cos(\Theta) \end{pmatrix} = \begin{pmatrix} 1 & 0 & 0 \\ 0 & \cos(\Theta) & -\sin(\Theta) \\ 0 & \sin(\Theta) & \cos(\Theta) \end{pmatrix}.$$

Then the transformation matrix for the ϕ rotation, which is the counter clock-wise rotation around the z axis, is

$$\begin{pmatrix} \cos(\Phi) & -\sin(\Phi) & 0 \\ \sin(\Phi) & \cos(\Phi) & 0 \\ 0 & 0 & 1 \end{pmatrix}.$$

Finally, the transformation matrix for the ψ counter clock-wise rotation around the y axis is:

$$\begin{pmatrix} \cos(\Psi) & 0 & -\sin(\Psi) \\ 0 & 1 & 0 \\ \sin(\Psi) & 0 & \cos(\Psi) \end{pmatrix}.$$

Thus the final transformation is

$$\begin{pmatrix} 1 & 0 & 0 \\ 0 & \cos(\Theta) & -\sin(\Theta) \\ 0 & \sin(\Theta) & \cos(\Theta) \end{pmatrix} \begin{pmatrix} \cos(\Phi) & -\sin(\Phi) & 0 \\ \sin(\Phi) & \cos(\Phi) & 0 \\ 0 & 0 & 1 \end{pmatrix} \begin{pmatrix} \cos(\Psi) & 0 & -\sin(\Psi) \\ 0 & 1 & 0 \\ \sin(\Psi) & 0 & \cos(\Psi) \end{pmatrix} \tag{1.7}$$

Assuming the angular movements are very small and multiplying the matrices we obtain the coordinate transformation

$$\begin{pmatrix} x \\ y \\ z \end{pmatrix} = \begin{pmatrix} L \\ Y(t) \\ Z(t) \end{pmatrix} + \begin{pmatrix} 1 & -\Phi & -\Psi \\ \Phi & 1 & -\Theta \\ \Psi & \Theta & 1 \end{pmatrix} \begin{pmatrix} \xi \\ \eta \\ \zeta \end{pmatrix}.$$

We will, for convenience, treat the rotating element as a disk of radius D. Any arbitrary point p on the disk has a polar representation with radius $\mathrm{r} \leq D$ and angle α, that angle measured in the

positive direction of the ζ, η plane, at nominal time $t = 0$. Let the angular rotation rate be $\omega(t)$. Then at time t we have

$$\xi(t) = r\cos(\alpha + \omega(t)),\ \ \eta(t)\ =\ r\sin(\alpha + \omega(t)),\ \ \zeta(t) = D.$$

In the inertial x, y, z plane we then have, for the cartesian coordinates of a point $X(t)$ lying on the rotating fan, suppressing the argument t,

$$X(t)\ =\ \begin{pmatrix} x \\ y \\ z \end{pmatrix}\ =\ \begin{pmatrix} L \\ Y(t) \\ Z(t) \end{pmatrix} + \begin{pmatrix} 1 & -\Phi & -\Psi \\ \Phi & 1 & -\Theta \\ \Psi & \Theta & 1 \end{pmatrix} \begin{pmatrix} \xi \\ \eta \\ \zeta \end{pmatrix} \tag{1.8}$$

Using polar representation of the ccoordinates of the points we have

$$\begin{aligned} X(t)\ &=\ \begin{pmatrix} x \\ y \\ z \end{pmatrix}\ =\ \begin{pmatrix} L \\ Y(t) \\ Z(t) \end{pmatrix} + \begin{pmatrix} 1 & -\Phi & -\Psi \\ \Phi & 1 & -\Theta \\ \Psi & \Theta & 1 \end{pmatrix} \begin{pmatrix} r\cos(\alpha+\omega) \\ r\sin(\alpha+\omega) \\ D \end{pmatrix} \\ &=\ \begin{pmatrix} L + r\cos(\alpha+\omega) - r\sin(\alpha+\omega)\Phi - D\Psi \\ Y(t) + r\cos(\alpha+\omega)\Phi + r\sin(\alpha+\omega)\Phi - D\Theta \\ Z(t) + r\cos(\alpha+\omega)\Psi + r\sin(\alpha+\omega)\Theta + D \end{pmatrix}. \end{aligned} \tag{1.9}$$

Holding α fixed, identifying Φ with $\sin\Phi$, 1 with $\cos\Phi$ and using trigonometric identities, then differentiating with respect to t , we have to first order, continuing to suppress the arguments (L, t),

$$\dot{X}(\alpha, r, t)\ =\ \begin{pmatrix} -r\ \sin(\alpha+\omega+\Phi)\left(\dot{\omega}+\dot{\Phi}\right)\ -\ D\,\dot{\Psi} \\ \dot{Y}\ +\ r\ \cos(\alpha+\omega+\Phi)\left(\dot{\omega}+\dot{\Phi}\right) - D\,\dot{\Theta} \\ \dot{Z} - \dot{\omega}r\ \sin(\alpha+\omega)\,\Psi + r\ \cos(\alpha+\omega)\,\dot{\Psi} + \dot{\omega}r\ \cos(\alpha+\omega)\,\Theta + r\ \sin(\alpha+\omega)\,\dot{\Theta} \end{pmatrix}. \tag{1.10}$$

In order to compute the fan kinetic energy

$$\frac{1}{2}\ \int_0^D\ m(r) \int_0^{2\pi} \|\dot{X}(\alpha, r, t)\|^2\, d\alpha\, r\, dr,$$

where $m(r)$ is the fan mass density per unit disc area (assumed independent of α) and D is the fan radius, we first compute the inner, α, integral, using the orthonormality of $\frac{1}{7}2\pi$, $\sin(\alpha+\omega)/\pi$, $\cos(\alpha+\omega)/\pi$ over the interval $0 \le \alpha \le 2\pi$, and then do the outer integral with the result

$$\begin{aligned} \int_0^{2\pi}\ \left\|\dot{X}(\alpha, r, t)\right\|^2\ d\alpha\ &=\ 2\,\pi\left[D^2\,\dot{\Psi}^2\ +\ \left(\dot{Y} - D\,\dot{\Theta}\right)^2 + \dot{Z}^2\right]\ + \\ &+\ \pi\, r^2\ \left[2\ \left(\dot{\omega}+\dot{\Phi}\right)^2 + \left(\dot{\Theta} - \dot{\omega}\,\Psi\right)^2 + \left(\dot{\omega}\Theta + \dot{\Psi}\right)^2\right]. \end{aligned}$$

Thus the kinetic energy of the fan is

$$\mathcal{T}_F\ \equiv\ \frac{M_F}{2}\left[D^2\left(\dot{\Psi}\right)^2\ +\ \left(\dot{Y} - D\,\dot{\Theta}\right)^2 + \left(\dot{Z}\right)^2\right]\ +$$

$$+\frac{I_F}{2}\left[2\left(\dot\omega+\dot\Phi\right)^2+\left(\dot\Theta-\dot\omega\,\Psi\right)^2+\left(\dot\omega\Theta+\dot\Psi\right)^2\right]. \tag{1.11}$$

where M_F is the mass of the fan and I_F is its moment of inertia about its center. All variables shown are assumed small except for $\dot\omega$.

In order to work entirely with small variables to obtain a linearized system we let

$$\dot\omega \;=\; \sigma \;+\; \dot{\delta\omega},$$

where σ denotes the (constant) nominal steady state fan rotation rate and $\dot{\delta\omega}$ denotes presumed small variations of the rotation rate about the value σ. Then, renaming $\dot{\delta\omega}$ as $\dot\omega$ again, (1.11) becomes

$$\mathcal{T}_F \;\equiv\; \frac{M_F}{2}\left[D^2\left(\dot\Psi\right)^2+\left(\dot Y-D\,\dot\Theta\right)^2+\left(\dot Z\right)^2\right]+$$
$$+\frac{I_F}{2}\left[2\left(\sigma+\dot\omega+\dot\Phi\right)^2+\left(\dot\Theta-(\sigma+\dot\omega)\,\Psi\right)^2+\left((\sigma+\dot\omega)\,\Theta+\dot\Psi\right)^2\right]. \tag{1.12}$$

In the second line here we retain only terms which are quadratic in the small variables; cubic and higher terms are simply discarded and linear and constant terms in the velocities disappear when Hamilton's principle is invoked. Thus

$$2\left(\sigma+\dot\omega+\dot\Phi\right)^2\;\to\;2\left(\dot\omega\;+\;\dot\Phi\right)^2,\qquad\left(\dot\Theta-(\sigma+\dot\omega)\,\Psi\right)^2\;\to\;\left(\dot\Theta-\sigma\,\Psi\right)^2,$$
$$\left((\sigma+\dot\omega)\,\Theta+\dot\Psi\right)^2\;\to\;\left(\sigma\,\Theta+\dot\Psi\right)^2.$$

Then we can replace (1.12) by

$$\mathcal{T}_F\;=\;\mathcal{T}_R\;+\;\mathcal{T}_\sigma\;=\;\frac{M_F}{2}\left[D^2\left(\dot\Psi\right)^2+\left(\dot Y-D\,\dot\Theta\right)^2+\left(\dot Z\right)^2\right]+$$
$$+\frac{I_F}{2}\left[2\left(\dot\omega+\dot\Phi\right)^2+\left(\dot\Theta-\sigma\,\Psi\right)^2+\left(\sigma\,\Theta+\dot\Psi\right)^2\right], \tag{1.13}$$

$\mathcal{T}_R$ denoting terms independent of σ and $\mathcal{T}_\sigma$ denoting those terms which involve σ.

Introducing the vector

$$Q(t)^*\;=\;(\,Y(t)\quad\Phi(t)\quad Z(t)\quad\Psi(t)\quad\Theta(t)\quad\omega(t)\,), \tag{1.14}$$

the kinetic energies due to rigid body motion of the generator head and fan can be expressed as quadratic forms in $\dot Q(t)$:

$$\mathcal{T}_H\;=\;\dot Q^*\mathbf{T}_H\,\dot Q;\quad\mathbf{T}_H\;=\;\mathrm{diag}\left(\frac{M_H}{2},\;\frac{I_{xz}}{2},\;\frac{M_H}{2},\;\frac{I_{xy}}{2},\;\frac{I_{yz}}{2},\;0\right),$$

$$\mathcal{T}_R\;=\;\dot Q^*\mathbf{T}_R\,\dot Q;\quad\mathbf{T}_R\;=\;\begin{pmatrix}\frac{M_F}{2}&0&0&0&-\frac{M_F\,D}{2}&0\\0&0&0&0&0&0\\0&0&\frac{M_F}{2}&0&0&0\\0&0&0&\frac{M_F\,D^2}{2}&0&0\\-\frac{M_F\,D}{2}&0&0&0&\frac{M_F\,D^2}{2}&0\\0&0&0&0&0&0\end{pmatrix}.$$

Finally, we have the rotational kinetic energy of the fan expressed in the form

$$\mathcal{T}_\sigma \,=\, \dot{Q}^*\mathbf{T}_{\sigma,1}\,\dot{Q} \,+\, \dot{Q}^*\mathbf{T}_{\sigma,2}\,Q \,+\, Q^*\mathbf{T}_{\sigma,3}\,Q,$$

where

$$\mathbf{T}_{\sigma,1} \,=\, \frac{I_f}{2}\begin{pmatrix} 0 & 0 & 0 & 0 & 0 & 0 \\ 0 & 2 & 0 & 0 & 0 & 2 \\ 0 & 0 & 0 & 0 & 0 & 0 \\ 0 & 0 & 0 & 1 & 0 & 0 \\ 0 & 0 & 0 & 0 & 1 & 0 \\ 0 & 2 & 0 & 0 & 0 & 2 \end{pmatrix},$$

$$\mathbf{T}_{\sigma,2} \,=\, \frac{I_F}{2}\,\mathrm{diag}\left(0,0,0,\begin{pmatrix} 0 & 2\,\sigma \\ -2\,\sigma & 0 \end{pmatrix},0\right) \qquad \mathbf{T}_{\sigma,3} \,=\, \frac{I_F}{2}\,\mathrm{diag}\left(0,0,0,\sigma^2,\sigma^2,0\right).$$

Combining $\mathbf{T} = \mathbf{T}_H + \mathbf{T}_R + \mathbf{T}_{\sigma,\,1}$ we have

$$\mathbf{T} \,=\, \begin{pmatrix} \frac{M_H}{2}+\frac{M_F}{2} & 0 & 0 & 0 & -\frac{M_F\,D}{2} & 0 \\ 0 & \frac{I_{xz}}{2}+I_F & 0 & 0 & 0 & I_F \\ 0 & 0 & \frac{M_H}{2}+\frac{M_f}{2} & 0 & 0 & 0 \\ 0 & 0 & 0 & \frac{I_{xy}}{2}+\frac{M_F\,D^2}{2}+\frac{I_F}{2} & 0 & 0 \\ -\frac{M_F\,D}{2} & 0 & 0 & 0 & \frac{I_{yz}}{2}+\frac{M_F\,D^2}{2}+\frac{I_F}{2} & 0 \\ 0 & I_F & 0 & 0 & 0 & I_F \end{pmatrix}.$$

1.3 Equations of Motion

It is straightforward to verify that Hamilton's principle leads to equations of motion of the combined generator head and fan, with F as in (1.14), take the form

$$\mathbf{T}\,\ddot{Q} \,+\, 2\,\mathbf{T}_{\sigma,2}\,\dot{Q} \,-\, \mathbf{T}_{\sigma,3}\;Q \,+\, F \,=\, 0. \tag{1.15}$$

It is worthwhile to note that if we make the change of independent variable $\tau = \sigma\,t$, continuing to treat σ as constant, then with $\mathbf{T}_{\sigma,\,2} \,=\, \sigma\,\mathbf{T}_2$, $\mathbf{T}_{\sigma,\,3} \,=\, \sigma^2\,\mathbf{T}_3$, the matrices $\mathbf{T}_2$, $\mathbf{T}_3$, are independent of σ and (1.15) becomes

$$\mathbf{T}\,\frac{d^2Q}{d\tau^2} \,+\, 2\,\mathbf{T}_2\,\frac{dQ}{d\tau} \,-\, \mathbf{T}_3\;Q \,+\, \frac{F}{\sigma^2} \,=\, 0. \tag{1.16}$$

This allows us to see that when σ is large the motions of the system are dominated by those of the homogeneous systems obtained from (1.16) by eliminating the last term, F/σ^2. This homogeneous system can be tentatively identified as the limit system as $\sigma \,\to\, \infty$, though further analysis will be required to confirm this identification.

The first order system corresponding to (1.15) can be written as

$$\frac{d}{dt}\begin{pmatrix} Q \\ \dot{Q} \end{pmatrix} \,=\, \begin{pmatrix} \mathbf{O} & \mathbf{I} \\ \mathbf{T}^{-1}\mathbf{T}_{\sigma,3} & -2\,\mathbf{T}^{-1}\mathbf{T}_{\sigma,2} \end{pmatrix}\begin{pmatrix} Q \\ \dot{Q} \end{pmatrix} + \begin{pmatrix} 0 \\ F \end{pmatrix}. \tag{1.17}$$

The components Φ and ω are uncoupled from the other components as far as the homogeneous version of this system is concerned but Y and Φ are coupled through their connection, via boundary conditions as noted below, to $y(x,\, t)$.

The overall Lagrangian, including the generator head, fan and supporting beam pylon, can now be taken to be

$$\mathcal{L} \equiv (\mathcal{T}_\sigma + \mathcal{T}_R + \mathcal{T}_H) + (\mathcal{T}_B - \mathcal{V}_B) \equiv \mathcal{L}_1 + \mathcal{L}_2,$$

$\mathcal{L}_1$ and $\mathcal{L}_2$ involving, respectively, $Q(t)$ and $q(x,\, t)$, where $Q(t)$ is given by (1.14) and

$$q(x,t) = \Big(y(x,t),\, z(x,t),\, \theta(x,t)\Big)^*.$$

We have already applied Hamilton's principle to $\mathcal{L}_1$ to obtain the equations for $Q(t)$ shown above. When we apply Hamilton's principle to $\mathcal{L}_2$, i.e.,

$$\frac{d}{dt}\frac{\partial \mathcal{L}_2}{\partial \dot{q}} - \frac{\partial \mathcal{L}_2}{\partial q} = 0,$$

with $\mathcal{L}_2 = \mathcal{T}_B - \mathcal{V}_B$,

$$\mathcal{V}_B = \int_0^L \left[\frac{k_y}{2}\left(\frac{\partial^2 y}{\partial x^2}(x,t)\right)^2 + \frac{k_z}{2}\left(\frac{\partial^2 z}{\partial x^2}(x,t)\right)^2 dx + \frac{k_\theta}{2}\left(\frac{\partial \theta}{\partial x}(x,t)\right)^2\right] dx, \tag{1.18}$$

$$\mathcal{T}_B = \int_0^L \left[\frac{M_B}{2}\left(\frac{\partial y}{\partial t}(x,t)\right)^2 + \frac{M_B}{2}\left(\frac{\partial z}{\partial t}(x,t)\right)^2 + \frac{I_B}{2}\left(\frac{\partial \theta}{\partial t}(x,t)\right)^2\right] dx, \tag{1.19}$$

we readily obtain the partial differential equations

$$M_B \frac{\partial^2 y}{\partial t^2} + \frac{\partial^2}{\partial x^2}\left(k_y \frac{\partial^2 y}{\partial x^2}\right) = 0, \tag{1.20}$$

$$M_B \frac{\partial^2 z}{\partial t^2} + \frac{\partial^2}{\partial x^2}\left(k_z \frac{\partial^2 z}{\partial x^2}\right) = 0, \tag{1.21}$$

$$I_B \frac{\partial^2 \theta}{\partial t^2} - \frac{\partial}{\partial x}\left(k_\theta \frac{\partial \theta}{\partial x}\right) = 0, \tag{1.22}$$

with the boundary conditions (1.5), (1.6). Further, the force/torque vector F in (1.15), (1.16) and (1.17) has components

$$F^* = \Big(F_Y,\, F_\Phi,\, F_Z,\, F_\Psi,\, F_\Theta,\, F_\omega\Big),$$

where, in the absence of exogenous effects such as wind gusts, etc.,

$$F_Y = k_y \frac{\partial^3 y}{\partial x^3}(L,t), \qquad F_\Phi = -k_y \frac{\partial^2 y}{\partial x^2}(L,t),$$

$$F_Z = k_z \frac{\partial^3 z}{\partial x^3}(L,t), \quad F_\Psi = -k_z \frac{\partial^2 z}{\partial x^2}, \quad F_\Theta = -k_\theta \frac{\partial \theta}{\partial x}(L,t). \tag{1.23}$$

The final component, F_ω, is zero until we consider varying wind torque, generator resistance, etc. We could clearly modify the forces (1.23) to include other effects such as damping, etc.

2 Adding Proofmass Actuators

A proof mass actuator, in the configuration which we will consider here, consists of an added mass, attached to the generator head, free to move along a channel, or "tube", in response to experienced acceleration from the motion of the generator head but also subject to restoring and frictional forces, the latter serving as an energy dissipator of the overall system.

2.1 Structure

We confine attention to proofmass actuators acting parallel to the y, z plane, along a line passing through the $x-$axis at $x = L + \ell$ in the direction corresponding to a unit vector $U = (0, U_y, U_z)$. We assume the guiding mechanism has mass $M_g > 0$ which, for simplicity, we assume located at $(L + \ell, 0, 0)$ in the equilibrium configuration. The proofmass, with mass M_p, has, in operation, respective first order y and z coordinates

$$Y(t) + \ell \sin(\Phi(t)) + p(t)U_y \approx Y(t) + \ell\Phi(t) + p(t)U_y,$$

$$Z(t) + \ell \sin(\Psi(t)) + p(t)U_z \approx Z(t) + \ell\Psi(t) + p(t)U_z,$$

where $p(t)$ denotes the displacement of the proof mass along its guiding channel. The corresponding velocity components, with an overdot (symbol) indicating the t derivative, are then

$$\dot{Y}(t) + \ell\,\dot{\Phi}(t) + \dot{p}(t)U_y, \quad \dot{Z}(t) + \ell\dot{\Phi}(t) + \dot{p}(t)U_z.$$

Thus the added kinetic energy term is

$$\frac{1}{2}M_p\left(\dot{Y}(t)^2 + \dot{Z}(t)^2\right) + \frac{1}{2}M_p\left(\left(\dot{Y}(t) + \ell\dot{\Phi}(t) + \dot{p}(t)U_y\right)^2 + \left(\dot{Z}(t) + \ell\dot{\Psi}(t) + \dot{p}(t)U_z\right)^2\right)$$

Additionally a term $\frac{1}{2}k_p p(t)^2$, where k_p is the assumed stiffness coefficient for the proofmass restoring mechanism, is added to the potential energy and an energy and an energy dissipation term $-\gamma\dot{p}(t)^2$, where $\gamma$is the proofmass coefficient of friction, is included.

The Q coordinates $Y, \Phi, Z, \Theta, \omega$, are augmented with p to form a seven dimensional vector which we will call Q_p. The added kinetic energy takes the form $\frac{1}{2}Q_p^* T_p Q_p$, where

$$T_p = m\begin{pmatrix} M_g + M_p & \ell(M_g + M_p) & 0 & 0 & 0 & 0 & M_pU_y \\ \ell(M_g + M_p) & \ell^2(M_g + M_p) & 0 & 0 & 0 & 0 & \ell M_pU_y \\ 0 & 0 & (M_g + M_p) & \ell(M_g + M_p) & 0 & 0 & M_pU_z \\ 0 & 0 & \ell(M_g + M_p) & \ell^2(M_g + M_p) & 0 & 0 & \ell M_pU_z \\ 0 & 0 & 0 & 0 & 0 & 0 & 0 \\ 0 & 0 & 0 & 0 & 0 & 0 & 0 \\ M_pU_y & \ell M_pU_y & M_pU_z & \ell M_pU_z & 0 & 0 & M_p \end{pmatrix} \tag{2.24}$$

The complete **T** matrix is then formed by adding a seventh column and seventh row of zeroes to the original **T** shown in (1.10), then adding (2.24) to the result. The change in the **V** matrix for the potential energy simply involves adding a zero row and a zero column to what we have discussed earlier, then placing k_p in the 7, 7 position. The complete system of equations is then obtained in the same manner as we have described in the previous section.

2.2 Tuning

The physical parameters of the proof mass actuator, as described here, must be carefully chosen, i.e., *tuned*, for effective vibration suppression in a multifrequency environment. At the time of completion of this thesis no theory fully adequate for use with our model has been developed. Related studies for simpler structures exist in the literature. The reader is referred to [6], [2] and [11] for studies carried out in relation to substantially simpler structures.

3 Splines

An important part of this thesis is computer simulation of the model presented in the previous sections. This clearly involves replacement of the partial differential equations modeling the supporting pylon by suitable discrete counterparts. Here we have elected to use spline based approximations, for which we now provide an introduction.

3.1 Introduction to Splines

Spline methods are designed to avoid the difficulties encountered when one tries to use a single polynomial to interpolate a large number of data points which occur naturally in continuous, infinite dimensional, systems. A response to this problem is to use piecewise polynomials. Historically, the design and construction of airplanes and ships involved the use of mechanical analogs. A method extensively used is to approximate a smooth path joining specified points was to take a thin, flexible metal strip, called a "spline" and bend it around pegs set at the required points. The resulting curves were traced out and used in the design. The curves that were traced out came to be known as splines. The most widely used splines involve piecewise cubic polynomials, but there is an extensive theory of splines involving piecewise polynomials of all orders.

3.2 Cubic Splines

Cubic splines use piecewise third-order polynomials which interpolate or approximate data at a set of k values of the independent variables, called nodes. The function values, derivatives and second derivatives of cubic splines are continuous over the whole domain. To see that we can require this in the interpolation context, let us assume that we have n data points represented by$((x_1, y_1), (x_2, y_2), \cdots, (x_n, y_n))$. Then we have $n-1$ intervals and, on each subinterval, four constants to determine a cubic polynomial on that interval. This provides us with $4(n-1)$ unknowns. At each x_k the data y_k must be matched, giving us n equations. In addition there are $n-2$ values x_k,$k = 2, 3, \cdots, n-1$, at which we must have continuity of the spline function and its first and second derivatives. this gives us $3(n-2)$ more equations. So, altogether, we have $4n-6$ equations for $4n-4$ unknowns. As we have indicated previously we obtain the remaining two equations by specifying the value of either the function or one of its first and second derivatives at each of the two end points of the interval. If, for example, the second derivative is set equal to zero at x_1 and x_n we obtain what are called the "natural splines". The calculation of the coefficients of the cubic polynomial on each subinterval is simplified by a suitable choice of the algebraic representation of the equations. In general, one does not require the spacing between x values to be equal. If this is required we obtain what are called "cardinal splines".

We let $h_i = x_{i+1} - x_i$. We look for a spline function of the form

$$S(x) = \begin{cases} P_1(x), x_1 \leq x \leq x_2, \\ P_i(x), x_i \leq x \leq x_{i+1} \\ P_{n-1}(x), x_{n-1} \leq x \leq x_n \end{cases}$$

For $i = 1, \cdots, n-1$, we write

$$P_i(x) = a_{i-1}\frac{(x_{i+1} - x)^3}{6h_i} + a_i\frac{(x - x_i)^3}{6h_i} + b_i(x_{i+1} - x) + c_i(x - x_i).$$

This form of the cubic is motivated by the fact that the second derivative of the polynomials on the adjacent subintervals must be equal at the common node between the two subintervals. Using the definition of the h_i, we can follow that $P_i^{''}(x_{i+1}) = a_i$ and that $P_{i+1}^{''}(x_{i+1}) = a_i$ also. Thus the form of expression for $P_i(x)$ensures that the second derivatives are continuous at the interior nodes. Next we integrate

$$P_i^n = a_{i-1}\frac{(x_{i+1} - x)}{h_i} + a_i\frac{(x - x_i)}{h_i}$$

twice and using the conditions that $P_i(x_i) = y_i$ and $P_i(x_{i+1}) = y_{i+1}$ we determine the values for the coefficients b_i and c_i and we can write the expression in the following form:

$$P_i(x) = a_{i-1}\frac{(x_{i+1} - x)^3}{6h_i} + a_i\frac{(x - x_i)^3}{6h_i}\left[y_i - \frac{a_{i-1}h_i^2}{6}\right]\frac{(x_{i+1} - x)}{6h_i} + \left[y_{i+1} - \frac{a_i h_i^2}{6}\right]\frac{(x - x_i)}{h_i}.$$

Now since the first derivatives of P_i and P_{i+1} must agree at x_{i+1} we deduce that

$$\frac{h_i}{6}a_{i-1} + \frac{h_i + h_{i+1}}{3}a_i + \frac{h_{i+1}}{6}a_{i+1} = \frac{y_{i+2} - y_{i+1}}{h_{i+1}} - \frac{y_{i+1} - y_i}{h_i}, i = 1, \cdots, n-2.$$

We now have $n-2$ equations and n unknowns. Even though we have many choices of specifying additional conditions, for a natural cubic spline we will assign $a_0 = a_{n-1} = 0$; i.e., the second derivative is zero at the end points x_1 and x_n. It is clear now that we have just enough conditions to just identify the system. The values of b_i and c_i where $i = 1, \cdots, n-1$ may be expressed in the following form

$$b_i = \frac{y_i}{h_i} - \frac{a_{i-1}h_i}{6}, \qquad c_i = \frac{y_{i+1}}{h_i} - \frac{a_i h_i}{6}.$$

3.3 Numerical Example for Cubic Splines

We consider the data points $(-2, 4)$, $(-1, -1)$, $(0, 2)$, $(1, 1)$ and $(2, 8)$. We take $h_i = 1$ for all intervals and we use the boundary conditions $a_0 = a_4 = 0$ for a natural cubic spline. Now the equations for a_1, a_2, and a_3 are as follows:

$$i = 1 : \frac{a_0}{6} + \frac{2a_1}{3} + \frac{a_2}{6} = (y_3 - y_2) - (y_2 - y_1);$$

$$i = 2 : \frac{a_1}{6} + \frac{2a_2}{3} + \frac{a_3}{6} = (y_4 - y_3) - (y_3 - y_2);$$

$$i = 3 : \frac{a_2}{6} + \frac{2a_3}{3} + \frac{a_4}{6} = (y_5 - y_4) - (y_4 - y_3);$$

After substituting the values for a_0, a_4, and $y_i (i = 1, \cdots, 5)$ and simplifying we obtain

$$4a_1 + a_2 = 48$$

$$a_1 + 4a_2 + a_3 = -24$$

$$a_2 + 4a_3 = 48$$

This gives us the tridiagonal system

$$\begin{bmatrix} 4 & 1 & 0 \\ 1 & 4 & 1 \\ 0 & 1 & 4 \end{bmatrix} \begin{bmatrix} a_1 \\ a_2 \\ a_3 \end{bmatrix} = \begin{bmatrix} 48 \\ -24 \\ 48 \end{bmatrix}.$$

We solve this system to obtain $a_1 = 15.42,\ a_2 = -13.71,\ a_3 = 15.42$. Then we solve for the b_i and we obtain

$$b_1 = y_1 - \frac{a_0}{6} = 4, b_2 = y_2 - \frac{a_1}{6} = -3.57, b_3 = y_3 - \frac{a_2}{6} = 4.28, b_4 = y_4 - \frac{a_3}{6} = -1.57,$$

and for the c_i we obtain

$$c_1 = y_2 - \frac{a_1}{6} = -3.57, c_2 = y_3 - \frac{a_2}{6} = 4.28, c_3 = y_4 - \frac{a_3}{6} = -1.57, c_4 = y_5 - \frac{a_4}{6} = 8.$$

Now we have identified all the coefficients of the system and we can express the cubic spline from the following final simplification [3].

$$S(x) = \begin{cases} 2.57(x+2)^3 - 4(x+1) - 3.57(x+2), -2 \le x \le -1, \\ -2.57x^3 - 2.29(x+1)^3 + 3.57x + 4.29(x+1), -1 \le x \le 0, \\ -2.29(1-x)^3 + 2.57x^3 + 4.29(1-x) - 1.57x, 0 \le x \le 1, \\ 2.57(2-x)^3 - 1.57(2-x) + 8(x-1), 1 \le x \le 2 \end{cases}$$

3.4 Cubic B-Splines

B-Splines, or *Basis Splines* are a generalization of the notion of a *Bėzier* curve. Such functions have very minimal support with respect to the degree, smoothness and domain partition while interpolating any given function. Cubic B-Splines are compactly supported cubic splines forming a basis for the vector space of general cubic splines. Normally, as we have seen earlier, we define cubic splines by an expression similar to

$$b_{k^3}^3 = \frac{1}{i_{k-1}} \int_{t_{k-2}}^{x} b_{k-1}^2(t)dt - \frac{1}{i_k} \int_{t_{k-1}}^{x} b_k^2(t)dt,$$

where

$$i_k = \int_{t_{k-1}}^{t_{k-2}} b_k^2(t)dt, \qquad i_{k-1} = \int_{t_{k-2}}^{t_{k+1}} b_{k-1}^2(t)dt.$$

The support of $b_k^3(x)$ will then be $[t_{k-2}, t_{k+2}]$. Now we set $b_k^3(x) = \alpha(x - t_{k-2})^3$ on the domain $[t_{k-2}, t_{k-1}]$. Then at t_{k-1} we have the value of the first and second derivative with respect to t_{k-1} to be $3\alpha(t_{k-1} - t_{k-2})^2, 6\alpha(t_{k-1} - t_{k-2})$ To match these, on $[t_{k-1}, t_k]$, we must have, approximating with Taylor's series,

$$b_k^3 = \alpha(t_{k-1} - t_{k-2})^3 + 3\alpha(t_{k-1} - t_{k-2})^2(x - t_{k-1}) + 3\alpha(t_{k-1} - t_{k-2})(x - t_{k-1})^2 + \beta(x - t_{k-1})^3$$

Now on $[t_{k+1}, t_{k+2}]$ we take $b_k^3(x) = \delta(x - t_{k-1})^3$. Obviously, the first and second derivatives are $-3\delta(t_{k+2} - x)^2, 6\delta(t_{k+2} - x)$. To match these values at t_{k+1} we define, on $[t_k, t_{k+1}]$,

$$b_k^3(x) = \delta(t_{k+1} - t_k)^3 - 3\delta(t_{k+2} - x)^2(t_{k+1} - x) + 6\delta(t_{k+2} - x)(t_{k+1} - x)^2 + \gamma(t_{k+1} - x)^3$$

Then at $x = t_k$, the value, the first and the second derivatives must agree. This would give us the following three equations

$$\alpha(t_{k-1} - t_{k-2})^3 + 3\alpha(t_{k-1} - t_{k-2})^2(t_k - t_{k-1}) + 3\alpha(t_{k-1} - t_{k-2})(t_k - t_{k-1})^2 + \beta(t_k - t_{k-1})^3$$

$$= \delta(t_{k+2} - t_{k+1})^3 + 3\delta(t_{k+2} - t_{k+1})^2(t_{k+1} - t_k) + 3\delta(t_{k+2} - t_{k+1})(t_{k+1} - t_k)^2 + \gamma(t_{k+1} - t_k)^3 \quad (3.25)$$

$$3\alpha(t_{k-1} - t_{k-2})^2 + 6\alpha(t_{k-1} - t_{k-2})(t_k - t_{k-1}) + 3\beta(t_k - t_{k-1})^2$$

$$= -3\delta(t_{k+2} - t_{k+1})^2 - 6\delta(t_{k+2} - t_{k+1})(t_{k+1} - t_k) - 3\gamma(t_{k+1} - t_k)^2 \quad (3.26)$$

$$6\alpha(t_{k-1} - t_{k-2}) + 6\beta(t_k - t_{k-1}) = 6\delta(t_{k+2} - t_{k+1}) + 6\gamma(t_{k+1} - t_k) \quad (3.27)$$

The above three equations can be solved for just three variables in order to just identify the system. The remaining variables can then be adjusted to according to the desired amplitude of b_k^3, i.e. the value of t_k. Assuming we have equally spaced knots with $h = 1$, we have the conditions

$$t_{k+1} - t_k = k = t_{k+2} - t_{k+1},$$

etc. Thus

$$6\alpha h + 6\beta h = 6\delta h + 6\gamma h \Rightarrow \alpha + \beta = \delta + \gamma$$

$$3\alpha h^2 + 6\alpha h^2 + 3\beta h^2 = -3\delta h^2 - 6\delta h^2 - 3\gamma h^2 \Rightarrow 9\alpha + 3\beta = -9\delta - 3\gamma$$

$$6\alpha + 6\beta = 6\delta + 6\gamma$$

We set $\alpha = \delta, \beta = \gamma$. It is obvious that the above choice of values satisfy our three spline equations above and its easy to deduce that

$$\alpha = -\frac{1}{3}\beta, \delta = -\frac{1}{3}\gamma$$

Therefore, for any value of α the following relation is true

$$(\alpha \quad \beta \quad \delta \quad \gamma) = (\alpha \quad -3\alpha \quad -3\alpha \quad \alpha).$$

Thus, for the spline function we have

$$b_k^3(x) = \alpha(x - t_{k-2})^3 = \alpha h^3 + 3\alpha h^2(x - t_{k-1}) + 3\alpha h(x - t_{k-1})^2 - 3\alpha(x - t_{k-1})^3$$

3.5 Numerical Example for Cubic B-Splines

On the interval $0 \leq x \leq 1$ we define the "knots" to be $t_k = .2k, k = 0, 1, 2, 3, 4, 5$ and we define the known y values to be $y_0 = 1, y_1 = \frac{3}{2}, y_2 = \frac{5}{2}, y_3 = \frac{1}{2}, y_4 = 3, y_5 = 2$. In order to determine the spline representation of the function represented by the given set of y_k points above the "knot" values can be immediately computed in the following manner.Assuming we take $\alpha h^3 = 1$, and the spline function as

$$S(x) = \sum_{k=-1}^{6} c_k \, b_k^3(x), \tag{3.28}$$

on $[t_{k-2}, t_{k-1}]$ we have the formula and the knot value at t_{k-2} :

$$b_k^3 = (x - t_{k-2})^3 = \frac{1}{h^3}(0) = 0.$$

Similarly, the other knot values can be computed to have the respective values $1, 4, 1$ and 0.

The support of b_k^3 is $[t_{k-2}, t_{k+2}]$ and is centered at t_k,. In order for $S(x)$, as given by (3.28), to have the indicated values at the given knots t_k it is clear that the c_k should satisfy the following system of 6 equations in 8 unknowns.

$$\begin{pmatrix} 1 & 4 & 1 & 0 & 0 & 0 & 0 & 0 \\ 0 & 1 & 4 & 1 & 0 & 0 & 0 & 0 \\ 0 & 0 & 1 & 4 & 1 & 0 & 0 & 0 \\ 0 & 0 & 0 & 1 & 4 & 1 & 0 & 0 \\ 0 & 0 & 0 & 0 & 1 & 4 & 1 & 0 \\ 0 & 0 & 0 & 0 & 0 & 1 & 4 & 1 \end{pmatrix} \begin{pmatrix} c_{-1} \\ c_0 \\ c_1 \\ c_2 \\ c_3 \\ c_4 \\ c_5 \\ c_6 \end{pmatrix} = \begin{pmatrix} 1 \\ 3/2 \\ 5/2 \\ 1/2 \\ 3 \\ 2 \end{pmatrix}, \quad \text{i.e., } \mathbf{B}\, C = F,$$

where $\mathbf{B}$, C and F are as follows

$$\mathbf{B} = \begin{pmatrix} 1 & 4 & 1 & 0 & 0 & 0 & 0 & 0 \\ 0 & 1 & 4 & 1 & 0 & 0 & 0 & 0 \\ 0 & 0 & 1 & 4 & 1 & 0 & 0 & 0 \\ 0 & 0 & 0 & 1 & 4 & 1 & 0 & 0 \\ 0 & 0 & 0 & 0 & 1 & 4 & 1 & 0 \\ 0 & 0 & 0 & 0 & 0 & 1 & 4 & 1 \end{pmatrix}, \; C = \begin{pmatrix} c_{-1} \\ c_0 \\ c_1 \\ c_2 \\ c_3 \\ c_4 \\ c_5 \\ c_6 \end{pmatrix}, \; F = \begin{pmatrix} 1 \\ 3/2 \\ 5/2 \\ 1/2 \\ 3 \\ 2 \end{pmatrix}.$$

We let $C = \mathbf{B}^* D$ and solve $\mathbf{B}\,\mathbf{B}^* D = F$ to obtain

$$D = \begin{pmatrix} .0544 \\ -.0230 \\ .2048 \\ -.1589 \\ .2151 \\ .0243 \end{pmatrix}, \qquad C = \mathbf{B}^* D = \begin{pmatrix} .0544 \\ .1946 \\ .1670 \\ .6372 \\ -.2157 \\ .7258 \\ .3125 \\ .0243 \end{pmatrix}.$$

Following our assumption of $\alpha h^3 = 1$ the values of the cubic B-Spline at the points $\frac{kh}{4}$ are readily seen to be ([14], [8])

$$\left(0, \quad \frac{1}{64}, \quad \frac{1}{8}, \quad \frac{27}{64}, \quad 1, \quad \frac{121}{64}, \quad \frac{23}{8}, \quad \frac{235}{64}, \quad 4, \quad \frac{235}{64}, \quad \cdots, \quad \frac{1}{64}, \quad 0\right) \equiv \beta$$

which has a total of 17 entries which are symmetric about 4. We can use these values to plot $S(x)$ on a grid finer than that corresponding to the t_k.

4 Spline Representation of the Dynamic Beam

Here we indicate how cubic and piecewise linear splines can be used to discretize the partial differential equations modeling the supporting pylon for our structure.

4.1 Spline Approximation of Partial Differential Equations

As an effort to discretize the model developed above, we begin with the cubic spline treatment of of the second order partial differential equation for the torsional displacement $\theta(x,t)$ of the supporting beam pylon. We begin this treatment by considering torsional displacement $\theta_\tau(x)$ due to a distributed torque $\tau(x)$ along with the boundary conditions $\theta_\tau(0) = 0, \theta_\tau(L) = \Theta$. In this case $\theta_\tau(x)$ is known to be solution of

$$min \int_0^L \left(\frac{1}{2} k_\theta(x) \left(\frac{d\theta}{dx}(x) \right)^2 - \tau(x)\theta(x) \right) dx \tag{4.29}$$

subject to the boundary conditions mentioned above. The minimum is taken over the set of functions $\theta(x)$ having square integrable derivatives on $[0, L]$.

Let us assume $k_\theta(x) \equiv k_\theta$ to be constant. Approximate the treatment of the above problem via cubic splines involves replacement of the set of functions $\theta(x)$ just described by the much more restricted set of "natural" cubic spline functions $\hat{\theta}(x)$,i.e., cubic splines whose second derivatives vanish at $x = 0$ and $x = L$. Assuming a partition

$$0 = x_0 < x_2 \cdots < x_{n-1} < x_n = L$$

of the interval $[0, L]$ with equally spaced knots of uniform separation $h = x_k - x_{k-1}, k = 1, 2, \cdots, n$ $\hat{\theta}(x)$ is taken to be a natural cubic spline function with knots $x_k, k = 1, 2, \cdots, n-1$, further satisfying the conditions

$$\hat{\theta}(0) = 0, \qquad \hat{\theta}(L) = \Theta. \tag{4.30}$$

We approximate the continuous torque $\tau(x)$ by a second order, i.e.,piecewise linear, spline $\hat{\tau}(x)$ with $\hat{\tau}(0) = \hat{\tau}(L) = 0$ and specified values at $x_k, k = 1, 2, \cdots, n-1$. Then one considers the discretized version of (4.29):

$$min \int_0^L \left(\frac{1}{2} k_\theta \left(\frac{d\hat{\theta}}{dx}(x) \right)^2 - \hat{\tau}(x)\hat{\theta}(x) \right) dx \tag{4.31}$$

In order to obtain necessary conditions for a minimum we introduce a small variation $\hat{\theta}(x) \rightarrow \hat{\theta}(x) + \delta\theta(x)$, where $\delta\theta(x)$ a natural cubic spline with $\delta\theta(0) = \delta\theta(L) = 0$. The first order variation in (4.31) is readily seen to be

$$\int_0^L \left(\left(\frac{1}{2} k_\theta \frac{d\hat{\theta}}{dx}(x) \frac{d\delta\theta}{dx}(x) \right)^2 - \hat{\tau}(x)\hat{\delta\theta}(x) \right) dx \tag{4.32}$$

Integrating the first term in the integrand by parts (4.32) becomes

$$-\int_0^L \left(k_\theta \left(\frac{d^2\hat{\theta}}{dx^2}(x) + \hat{\tau} \right) \delta\theta(x)dx + k_\theta \frac{d\hat{\theta}}{dx}(x)\delta\theta(x) \right) dx \tag{4.33}$$

Since $\delta\theta(0) = \delta\theta(L) = 0$ the boundary terms in (4.33) disappear. Then, in order for (4.33) to vanish for all $\delta\theta(x)$ as has been indicated , it is both necessary and sufficient that

$$k_\theta \frac{\partial^2\hat{\theta}}{\partial x^2}(x) + \hat{\tau}(x) = 0, \qquad x \in [0, L] \tag{4.34}$$

Since both terms on the left are second order splines vanishing at $x = 0$ and $x = L$ they are completely and uniquely determined by their values at the knots x_k, $k = 1, 2, \cdots, n-1$. We conclude that (4.34) is equivalent to

$$k_\theta \frac{\partial^2\hat{\theta}}{\partial x^2}(x_k) + \hat{\tau}(x_k) \equiv 0, \qquad k = 1, 2, \cdots, n-1 \tag{4.35}$$

These equations, together with (4.31), constitute the natural spline "collocation" method for approximate solution of the minimization problem (4.29) for a given distributed torque $\tau(x)$. The corresponding approximation method for solution of (reference)is obtained by replacing $\tau(x)$ with inertial torque corresponding to the torsional acceleration term

$$I_B \frac{\partial^2\hat{\theta}}{\partial t^2}(x_k, t) - k_\theta \frac{\partial^2\hat{\theta}}{\partial x^2}(x_k, t) = 0, \tag{4.36}$$

again used together with (4.31). The partial derivatives $\frac{\partial^2\hat{\theta}}{\partial t^2}(x_k, t)$ are, of course, readily computed from the natural cubic spline form of $\hat{\theta}(x, t)$. The torque acting at $x = x_n = L$ is then $-k_\theta \frac{\partial\hat{\theta}}{\partial x}(L, t)$ which results in the third equation of motion being replaced by

$$F_\Theta = -k_\theta \frac{\partial\hat{\theta}}{\partial x}(L, t); \tag{4.37}$$

where the partial derivative $\frac{\partial\hat{\theta}}{\partial x}(L, t)$ is readily computed from the form of $\hat{\theta}(x)$.

An alternative to the above, which serves in part to motivate the approach we have taken in the sequel,is to take $\hat{\theta}(x)$ to be second order, piecewise linear, spline instead of a natural spline. The computations that follow proceed much as above except that the torque $\tau(x)$ is represented by discrete values τ_k, $k = 1, 2, \cdots, n-1$, and (4.32) is replaced by

$$min \left(\int_0^L \frac{1}{2} k_\theta \left(\frac{d\hat{\theta}}{dx}(x) \right) dx - h \sum_{k=1}^{n-1} \tau_k \hat{\theta}(x_k) \right) \tag{4.38}$$

and the variation (4.33)becomes

$$min\left(\int_0^L k_\theta \frac{d\hat{\theta}}{dx}(x)\frac{d\delta\theta}{dx}(x)dx - h\sum_{k=1}^{n-1}\tau_k\delta\theta(x_k)\right) \tag{4.39}$$

Integrating by parts on each interval (x_{k-1}, x_k), $k = 1, 2, \cdots, n-1$ and using the fact that $\frac{\partial^2\hat{\theta}}{\partial x^2} \equiv 0$ we obtain

$$\int_0^L k_\theta \frac{d\hat{\theta}}{dx}(x)\frac{d\delta\theta}{dx}dx = k_\theta\sum_{k=1}^{n}\frac{d\hat{\theta}}{dx}(x)\delta\theta(x) \tag{4.40}$$

$$= k_\theta\sum_{k=1}^{n}\left(\frac{d\hat{\theta}}{dx}(x_{k^-})\delta\theta(x_{k^-}) - \frac{d\hat{\theta}}{dx}(x_{k-1^+})\delta\theta(x_{k-1^+})\right)$$

$$= k_\theta\sum_{k=1}^{n-1}\frac{\hat{\theta}(x_k)-\hat{\theta}(x_{k-1})}{h}\left(\delta\theta(x_k)-\delta\theta(x_{k-1})\right).$$

Using the fact that $\delta\theta(0) = \delta\theta(L) = 0$ and re-ordering the summation the above becomes

$$-k_\theta\sum_{k=1}^{n}\frac{\hat{\theta}(x_{k+1})-2\hat{\theta}(x_k)+\hat{\theta}(x_{k-1})}{h}\delta\theta(x_k) = 0.$$

So that setting the variation (4.39) equal to zero yields

$$-k_\theta\sum_{k=1}^{n}\frac{\hat{\theta}(x_{k+1})-2\hat{\theta}(x_k)+\hat{\theta}(x_{k-1})}{h}\delta\theta(x_k) + \tau_k = 0,.$$

Since this must be true for all $\delta\theta(x_k)$ we obtain the equations

$$\frac{\hat{\theta}(x_{k+1})-2\hat{\theta}(x_k)+\hat{\theta}(x_{k-1})}{h} + \tau_k = 0 \quad k = 1, 2, \cdots, n-1.$$

In application to the time dependent wave equation the τ_k are replaced by the inertial torques $-hI_B\frac{\partial^2\hat{\theta}}{\partial x^2}(x_k, t)$ and the collocation method based on linear splines becomes

$$I_B\frac{\partial^2\hat{\theta}}{\partial x^2}(x_k,t) - \frac{\hat{\theta}(x_{k+1})-2\hat{\theta}(x_k)+\hat{\theta}(x_{k-1})}{h^2} = 0, k = 1, 2, \cdots, \quad k = 1, 2, \cdots, n-1. \tag{4.41}$$

Finally, we discretize the Euler - Bernoulli beam equations (1.20), (1.21) by using cubic splines. Since the Euler-Bernoulli beam equations and the asssociated boundary conditions are identical it will be sufficient to consider (1.20). We begin this analysis with the static problem for constant k_y again. The problem boils down to the following when we incorporate the boundary conditions

$$k_y\frac{\partial^4 y}{\partial x^4} = f(x), \quad y(0) = \frac{dy}{dx}(0) = 0, \quad y(L) = Y, \quad y'(L) = \Phi \tag{4.42}$$

These equations are combined with necessary conditions for the problem

$$min\int_0^L\left(\frac{k_y}{2}\left(\frac{d^2y}{dx^2}\right)^2 - f(x)y(x)\right)dx$$

over an appropriate set of functions $y(x)$, $f(x)$ being an applied force function. The related cubic spline function method restricts the set of admissible functions to cubic splines (not just "natural" cubic splines) $\hat{y}(x)$ on the interval $[0, L]$ which satisfy the same boundary conditions as shown in (4.42) and have knots at the points x_k, $k = 1, 2, \cdots, n-1$, as discussed earlier. Then the modified minimization problem is

$$min \left\{ \int_0^L \frac{k_y}{2} \left(\frac{d^2\hat{y}}{dx^2}(x) \right)^2 dx - h \sum_{k=1}^{n-1} f_k \hat{y}(x_k) \right\} \tag{4.43}$$

for discrete lateral force values f_k, $k = 1, 2, \cdots, n-1$. Considering a variation $\hat{y}(x) \to \hat{y}(x) + \delta y(x)$, where $\delta y(x)$ is a cubic spline with $\delta y(0) = \delta y(L) = 0, \frac{d\delta y}{dx}(0) = \frac{d\delta y}{dx}(L) = 0$, we obtain the variation of the integral in (4.43)in the form

$$k_y \int_0^L \frac{d^2\hat{y}}{dx^2}(x) \frac{d^2\delta y}{dx^2}(x) dx.$$

Integrating by parts and taking account of the boundary conditions on $\delta y(x)$ the variation of the integral becomes

$$-k_y \int_0^L \frac{d^3\hat{y}}{dx^3}(x) \frac{d\delta y}{dx}(x) dx = -k_y \sum_{k=1}^{n-1} \int_{x_{k-1}}^{x_k} \frac{d^3\hat{y}}{dx^3}(x) \frac{d\delta y}{dx}(x) dx \tag{4.44}$$

Now we apply integration by parts separately to each integral on the right hand side of (4.44) and use $\frac{d^4\hat{y}}{dx^4}(x) \equiv 0$ on each interval (x_{k-1}, x_k) to see that

$$k_y \int_{x_{k-1}}^{x_k} \frac{d^3\hat{y}}{dx^3}(x) \frac{d\delta y}{dx}(x) dx = k_y \left(\frac{d^3\hat{y}}{dx^3}(x_k) \delta y(x_k) - \frac{d^3\hat{y}}{dx^3}(x_{k-1}) \delta y(x_{k-1}) \right)$$

Going back through (4.43) and (4.44), rearranging the sum in the latter, the necessary condition for solution of the former is

$$\sum_{k=1}^{n-1} \left(k_y \left(\frac{d^3\hat{y}}{dx^3}(x_k+) - \frac{d^3\hat{y}}{dx^3}(x_k-) \right) - h f_k \right) \delta y(x_k) = 0, \quad k = 1, 2, \cdots, n-1$$

Since the variations $\delta y(x_k)$, $k = 1, 2, \cdots, n-1$, are independent we conclude that

$$k_y \left(\frac{d^3\hat{y}}{dx^3}(x_k+) - \frac{d^3\hat{y}}{dx^3}(x_k-) \right) - h f_k = 0, \quad k = 1, 2, \cdots, n-1. \tag{4.45}$$

The formula (4.45) then constitutes the cubic spline collocation method for solution of (4.42). For the time dependant problem we replace the f_k by the discretized inertial forces $-M_B \frac{d^2}{dt^2}(x_k)$ to obtain the differential equations which constitute the cubic spline collocation method for (1.20), (1.21):

$$M_B \frac{d^2}{dt^2}(x_k, t) + \frac{k_y}{h} \left(\frac{d^3\hat{y}}{dx^3}(x_k+, t) - \frac{d^3\hat{y}}{dx^3}(x_k-, t) \right) = 0, \quad k = 1, 2, \cdots, n-1. \tag{4.46}$$

The relevant boundary conditions on $y(x, t)$ are shown in (4.42). The terms in (reference) due to coupling of $y(x, t)$ with $Y(t)$ and $\Phi(t)$ are

$$F_Y(t) = k_y \frac{d^3y}{dx^3}(L, t), \qquad F_\Phi(t) = -k_y \frac{d^2y}{dx^2}(L, t). \tag{4.47}$$

4.2 Computation of Derivatives

The method (4.41) can be implemented directly because the second time derivative of the approximate solution is given directly in terms of the discretized state. This is not the case for the two methods based on cubic splines where x derivatives of the spline representation of the current state must be computed. We will treat the problem of derivative computation for (4.37) and (4.46) in that order. Some of this material is common to the two cases; we use $\hat{y}$ as the dependent variable in that part of the discussion. We extend the set of partition points by defining

$$x_k \,=\, kh, \quad k \,=\, -1, 0, 1, \cdots, n, n+1,$$

$n+3$ points in all. This is a purely mathematical device with no implications for extension of the physical system being modeled. For each such value of k we denote the cubic B-spline centered at x_k with uniform knot separation h by $b_k^3(x)$ and we normalize in a way so that the successive knot values are $0, 1, 4, 1, 0$. We suppress the t variable for now and assume the representation

$$\hat{y}(x) \,=\, \sum_{k=-1}^{n+1} c_k b_k^3(x). \tag{4.48}$$

We denote the $n+3-$dimensional vectors whose components are c_k by C. Arising from the interpolation and zero order boundary conditions we have $n+1$ equations

$$c_{k-1} + 4c_k + c_{k+1} \,=\, \hat{y}_k, \quad k \,=\, -1, 0, 1, \cdots, n. \tag{4.49}$$

In order to identify the system we should have two more independent conditions to solve for C.

In the particular case of (4.37), where the independent variable is $\hat{\theta}$ there are no further boundary conditions and the further two conditions arise from the requirement that $\hat{\theta}(x)$ should be a *natural* cubic spline, i.e.,

$$\frac{d^2\hat{\theta}}{dx^2}(0) \,=\, \frac{d^2\hat{\theta}}{dx^2}(L) \,=\, 0.$$

Since the knot values of the second derivatives for the cubic splines as specified are $0, \frac{6}{h^2}, -\frac{12}{h^2}, \frac{6}{h^2}, 0$, the two additional equations in this case can be taken to be (after dividing by 6)

$$\frac{1}{h^2}c_{-1} - \frac{2}{h^2}c_0 + \frac{1}{h^2}c_1 \,=\, 0, \quad \frac{1}{h^2}c_{n-1} - \frac{2}{h^2}c_n + \frac{1}{h^2}c_{n+1} \,=\, 0 \tag{4.50}$$

As shown, e.g., in [8][KinChen], the joint system (4.49), (with $\hat{y}$ replaced by $\hat{\theta}$) (4.50) is uniquely solvable, giving C in the form

$$C \,=\, \mathbf{C}\,\hat{\Theta} + D\,\Theta, \tag{4.51}$$

where $\mathbf{C}$ is an $(n+3)\times(n-1)$ matrix, $\hat{\Theta}$ is the $n-1-$dimensional vector whose components are the $\hat{\theta}_k$, $k \,=\, 1, 2, \cdots, n-1.$, D is an $n+3-$dimensional vector and Θ is the (scalar) rotational component

of the generator head in the y, z plane as introduced earlier. Once C, D have been obtained we have the second derivatives needed in (4.37) in the form

$$\frac{\partial^2\hat{\theta}}{\partial x^2}(x_k) \;=\; \frac{6}{h^2}c_{k-1} - \frac{12}{h^2}c_k + \frac{6}{h^2}c_{k+1}, \quad k \;=\; 1, 2, \cdots, n-1,$$

which in view of (4.51), gives these second derivatives in terms of $\hat{\Theta}$ and Θ.

To calculate the differences of third derivatives needed in (4.46) we note that the third derivatives of $b_k^3(x)$ are constant on subintervals (x_{j-1}, x_j) and have the values

$$\frac{d^3}{dx^3}b_k^3(x) \;=\; \begin{cases} 0, \quad \mathrm{x} \in (\mathrm{x_{j-1}}, \mathrm{x_j}), \mathrm{j} \leq \mathrm{k}-2, \\ 6/h^3, \quad x \in (x_{k-2}, x_{k-1}), \\ -18/h^3, \quad x \in (x_{k-1}, x_k), \\ 18/h^3, \quad x \in (x_k, x_{k+1}), \\ -6/h^3, \quad x \in (x_{k+1}, x_{k+2}), \\ 0, \quad x \in (x_{j-1}, x_j), j \geq k+3. \end{cases}$$

Accordingly, then, we have

$$\frac{1}{h}\left(\frac{d^3}{dx^3}b_k^3(x_j) - \frac{d^3}{dx^3}b_k^3(x_{j-1})\right) \;=\; \begin{cases} 6/\mathrm{h}^4, \quad \mathrm{j} \leq \mathrm{k}-2, \\ -24/h^4, \quad j \;=\; k-1, \\ 36/h^4, \quad j \;=\; k \\ -24/h^4, \quad j \;=\; k+1, \\ 6/h^4, \quad j \;=\; k+2. \end{cases} \tag{4.52}$$

Assuming the representation (4.48) we can see from (4.52) that, for $k \;=\; 1, 2, \cdots, n-1$,

$$\frac{1}{h}\left(\frac{d^3}{dx^3}\hat{y}(x_k+) - \frac{d^3}{dx^3}\hat{y}(x_k-1)\right) \;=\; \frac{1}{h^4}(6c_{k-2} - 24c_{k-1} + 36c_k - 24c_{k+1} + 6c_{k+2}). \tag{4.53}$$

We express c_k in terms of the $\hat{y}_j$, Y and Φ much as in the earlier case and we continue to have (4.49), which brings the value of Y for $k \;=\; n$. However, in this case the natural spline equations (4.50) do not apply; instead the first derivatives are specified at $x \;=\; 0,$ Ł. From this we can deduce that

$$\frac{d^3}{dx^3}b_k^3(x_j) \;=\; \begin{cases} 0, \quad j \;=\; k-2, \\ 3/h, \quad j \;=\; k-1, \\ 0, \quad j \;=\; k, \\ -3/h, j \;=\; k+1, \\ 0, \quad j \;=\; k+2 \end{cases}$$

Therefore, the boundary conditions $\frac{d\hat{y}}{dx}(0) \;=\; 0, \quad \frac{d\hat{y}}{dx}(L) \;=\; \Phi$ correspond to the conditions

$$\frac{3}{h}(c_1 - c_{-1}) \;=\; 0, \quad \frac{3}{h}(c_{n+1} - c_{n-1}) \;=\; \Phi.$$

These replace (4.50) and together with (4.49), which now includes the condition $\hat{y}(L) \;=\; Y$, we have a total of $n+3$ equations again. These equations are solvable to give, instead of (4.51), a vector equation of the form

$$C \;=\; \tilde{\mathbf{C}}\hat{\mathbf{Y}} + \tilde{\mathbf{D}}\mathbf{Y} + \tilde{\mathbf{E}}\mathbf{\Phi}, \tag{4.54}$$

where C, as before, is an $(n+3)-$dimensional vector, $\tilde{\mathbf{C}}$ is an $(n+3) \times (n-1)$ matrix, $\hat{Y}$ is the $(n-1)-$dimensional vector whose components are the $\hat{y}_k$ and $\tilde{D}$, $\tilde{E}$, are $(n+3)-$dimensional

vectors. The components $c_k, \quad k = -1, 0, 1, \cdots, n, n+1$, of C are thereby determined. Substituted into (4.53) and then into (4.46) we then have the cubic spline collocation method for the elastic beam with our boundary conditions.

Before we end this section, it is worthwhile to note that it is not absolutely necessary to represent cubic, or other, splines in terms of B-splines; the latter is primarily advantageous as a cure for ill-conditioning in high dimensional (n large) computations. Where this is not a problem , typically the case where n, the number of subintervals of $[0, L]$, is modest, one may also express cubic spline functions $s(x)$, $x \in [x_{k-1}, x_k]$, as

$$s(x) = a_k + b_k(x - x_{k-1}) + \frac{c_k}{2}(x - x_{k-1})^2 + \frac{d_k}{6}(x - x_{k-1})^3, \tag{4.55}$$

using $4n$ coefficients $a_k, b_k, c_k, d_k, \quad k = 1, 2, \cdots, n$. Assuming equal subintervals of length $h = L/n$, the consistency conditions become, for $k = 1, 2, \cdots, n-1$,

$$a_{k+1} = a_k + b_k h + \frac{c_k}{2}h^2 + \frac{d_k}{6}h^3,$$

$$b_{k+1} = b_k + c_k h + \frac{d_k}{2}h^2,$$

$$c_{k+1} = c_k + d_k h,$$

a total of $3n - 3$ linear equations. The interpolation requirements for given $y_0, y_1, \cdots, y_n$ are

$$a_k = y_{k-1}, \quad k = 1, 2, \cdots .n-1, a_n + b_n h + \frac{c_n}{2}h^2 + \frac{d_n}{6}h^3 = y_n,$$

altogether $n+1$ linear equations for a total now of $4n-2$. The remaining two conditions depend on the problem at hand. For natural cubic splines one uses

$$\frac{d^2 s}{dx^2}(0) = c_1 = 0, \qquad \frac{d^2 s}{dx^2}(L) = c_n + d_n h = 0,$$

and the spline function $s(x)$ is then completely determined. For application to our Euler- Bernoulli beam equations with clamped end points one would, instead, use

$$\frac{ds}{dx}(0) = b_1 = 0, \qquad \frac{ds}{dx}(L) = b_n + c_n h + \frac{d_n}{2}h^2 = 0.$$

Clearly, the expression of derivatives of $s(x)$ at the knots x_k is considerably simpler via this approach; the second derivatives of $s(x)$ at the internal knots are directly expressed as

$$\frac{d^2(s)}{dx^2}(x_k) = c_{k+1}, \quad k = 1, 2, \cdots, n-1.$$

4.3 Solving the Approximating ODEs

Let us denote by W the total system vector consisting of the $y_k, \quad z_k, \quad \theta_k, \quad k = 1, 2, \cdots, n-1$, arising from spline modeling of the beam structure as well as the components Y, Φ, Z, Ψ, Θ and ω

together with the corresponding velocities of these $3(n-1)+6$ components. Whatever method is used for discretization with respect to the x variable, as described in the previous section, the resulting spatially discretized system will be a first order linear system of dimension $6(n-1)+12$ taking the form

$$\frac{dW}{dt} = \mathbf{A}\mathrm{W}, \qquad \mathrm{t} \geq 0,$$

wherein $\mathbf{A}$ is a $(6(n-1)+12)\times(6(n-1)+12)$ matrix. In order to carry out a computer simulation this system of linear differential equations, continuous in time, must be replaced by a timewise discrete system. In our system we have chosen to use a modified trapezoidal rule for this purpose. We will suppose initial data vector W_0 given at $t = t_0 = 0$. We subdivide the interval $t > 0$ into subintervals of equal step length g. Approximations W_k to the solution W at $t = t_k$ are generated by the implicit formula.

$$W_{k+1} = W_k + g\mathbf{A}\ \ (\alpha \mathrm{W_k} + \beta \mathrm{W_{k+1}}), \quad \mathrm{k} = 1, 2, \cdots.$$

where α, β are positive numbers with $\alpha + \beta = 1$. The standard trapezoidal method corresponds to $\alpha = \beta = 1/2$. After the necessary algebraic manipulation we obtain the explicit formula

$$W_{k+1} = (\mathbf{I} - \beta \mathrm{g}\mathbf{A})^{-1}(\mathbf{I} + \alpha \mathrm{g}\mathbf{A})\mathrm{W_k} \equiv \mathbf{M}(\alpha, \beta)\mathrm{W_k}, \quad \mathrm{k} = 0, 1, 2, \cdots.$$

From the matrix *spectral mapping theorem* for matrices [4], if for $l = 1, 2, \cdots, 6(n-1)+12$ the eigenvalues of the matrix $\mathbf{A}$ are λ_l (for simplicity we assume there is a basis of eigenvectors), then the corresponding eigenvalues of $\mathbf{M}(\alpha, \beta)$ are

$$\mu_l = \frac{1 + \alpha g \lambda_l}{1 - \beta g \lambda_l}, \quad l = 1, 2, \cdots, 6(n-1)+12.$$

For purely imaginary $\lambda_l = i\nu_l$ as arise from our system in the stable instances, we readily find that

$$|\mu_l| = \sqrt{\frac{1 + \alpha^2 g^2 \nu_l^2}{1 + \beta^2 g^2 \nu_l^2}}, \quad l = 1, 2, \cdots, 6(n-1)+12.$$

Clearly, we have $|\mu_l| = 1$ for all l just in case $\alpha = \beta = 1/2$. This corresponds to the stability of the numerical method for the case of the standard trapezoidal rule. For numerical reasons, however, in practice it is usually best to use a value of β just a little larger than α; we have used $\alpha = .4999999, \ \ \beta = .5000001$ in our computations as outlined in the next section.

5 Computer Simulation Results

The model developed in §1 and §2 was coded for computer simulation and studied extensively during the development of this thesis. The Matlab$^{(R)}$ program used for the simulation allowed user specification of n, the number of subintervals of $[0, L]$ used in cubic spline representation, and the various structural parameters. After extensive experimentation it was determined that $n = 4$ provided sufficient structural flexibility in analysis of the supporting pylon. This allowed use of the alternate spline representation (4.55) without encountering any ill-conditioning problems or loss of accuracy.

The structural parameters used in this study were

$$\begin{array}{ccc} k_y = 10; & k_z = 10; & k_\theta = 10; \\ M_B = 1; & M_H = 2; & M_F = 2; \\ I_{x\,y} = 1; & I_{x\,z} = 1; & I_{y\,z} = 1; \\ & I_B = 1; & \\ I_F = 2; & L = 10; & D = 1. \end{array}$$

In addition there is the nominal wind fan rotation speed parameter σ whose variation corresponds to the different operational conditions; we will indicate the specification of σ as appropriate in the sequel.

With these parameter values a series of careful simulations has shown that the critical value of σ is approximately $\sigma_1 \equiv 1.07926$. For $\sigma < \sigma_1$ all eigenvalues of the overall system are either 0 or purely imaginary; solution trajectories are bounded in terms of initial data. It is clearly not

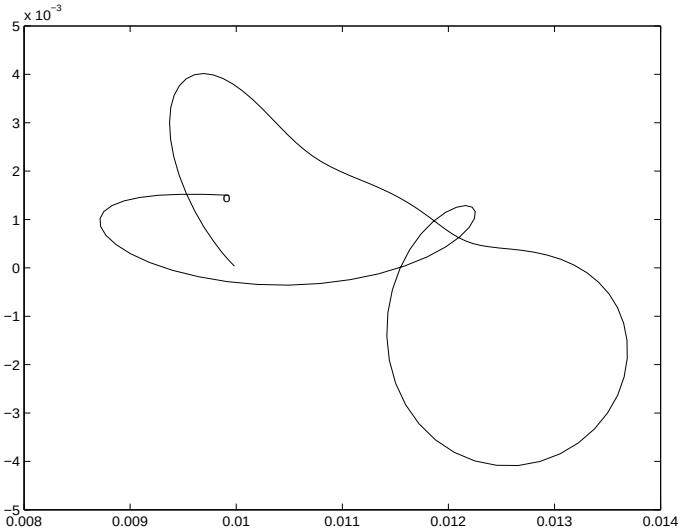

Figure 1: Ψ vs Θ trajectory for $\sigma = 1$.

feasible to show the complete trajectory for a system of dimension $6(n-1)+12$ or larger. Since we are interested primarily in possible oscillations of the fan axis about equilibrium we have selected the angles $\Psi(t)$ and $\Theta(t)$ for display. We begin with $\sigma = 1 < \sigma_1$. Here with purely imaginary

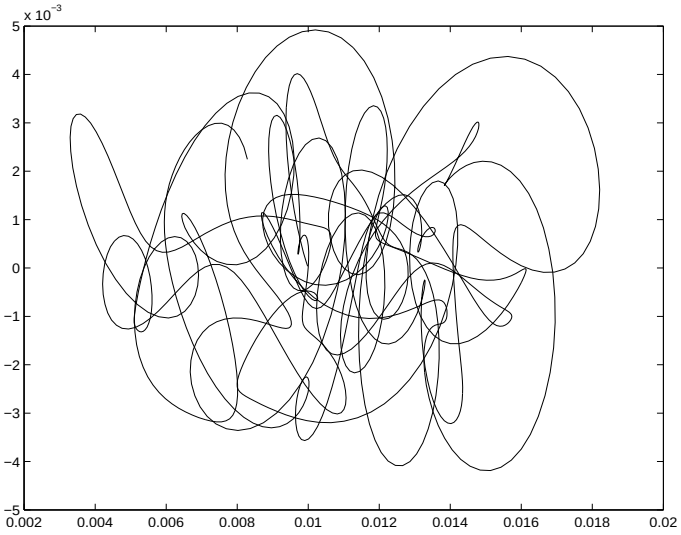

Figure 2: Extended Ψ vs Θ trajectory for $\sigma = 1$.

system eigenvalues we display the bounded time behavior of these variables, for given small initial system data, in Figures 1 and 2, the latter figure simply showing a longer time interval than the first. The semi-chaotic appearance of the trajectories in Figure 2 is accounted for by the influence of coupling to the elastic pylon structure which vibrates with a large number of modes in a wide range of frequencies. In Figure 3 we show the eigenvalues for the case $n = 4,\ \sigma = 1$ discussed above.

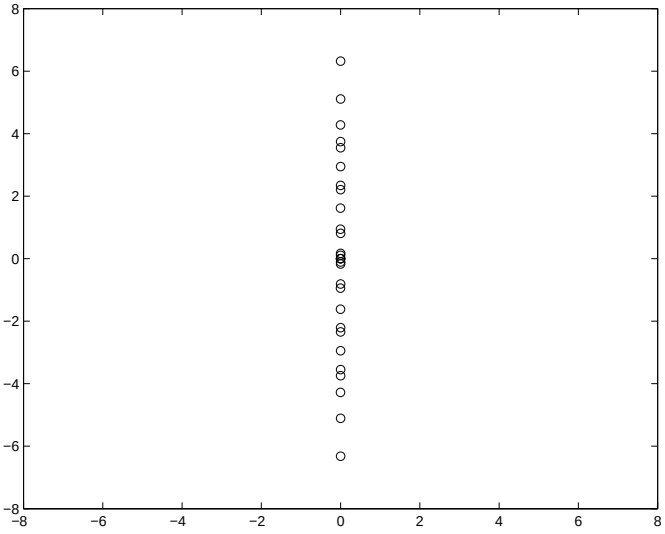

Figure 3: Eigenvalues for $\sigma = 1$

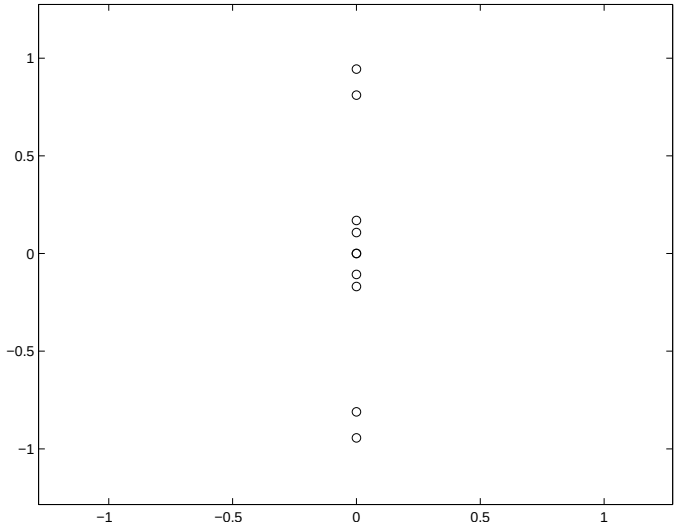

Figure 4: Enlarged view of spectrum near origin.

Next we move on to a slightly higher value of σ, very close to the critical frequency σ_1. We plot over a much longer time interval and we obtain Figure 5. Then going on to $\sigma = 1.08$ we obtain the spiral pattern shown in Figure 4. This is clearly unrealistic from a physical point of view as, continued, it would imply an unbounded state.

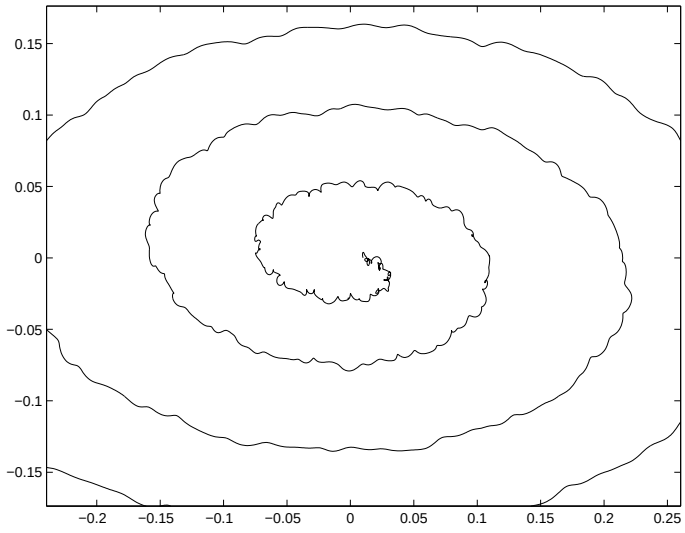

Figure 5: Ψ vs Θ trajectory for critical value of σ.

As we increase σ above the critical value eigenvalues with non-zero real part begin to appear. In the present case these appear in pairs, as shown in Figure 6

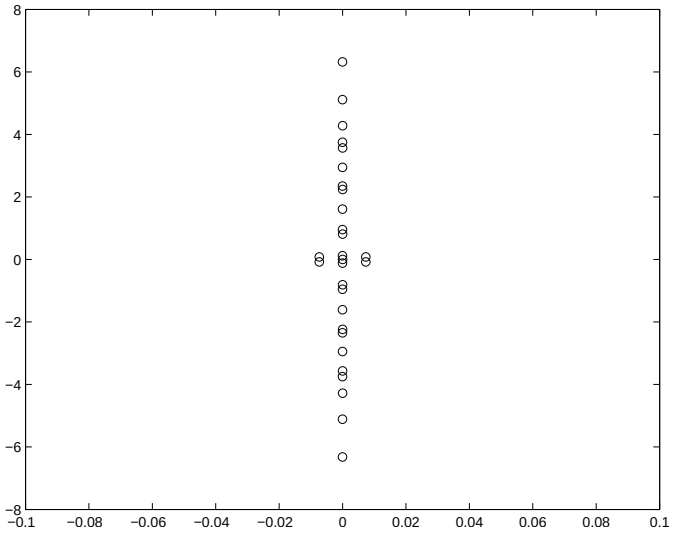

Figure 6: Eigenvalues for super-critical value $\sigma = 1.08$.

As a consequence trajectories now become unbounded as we see in Figure 7. This is, of course, unphysical and requires some remediation.

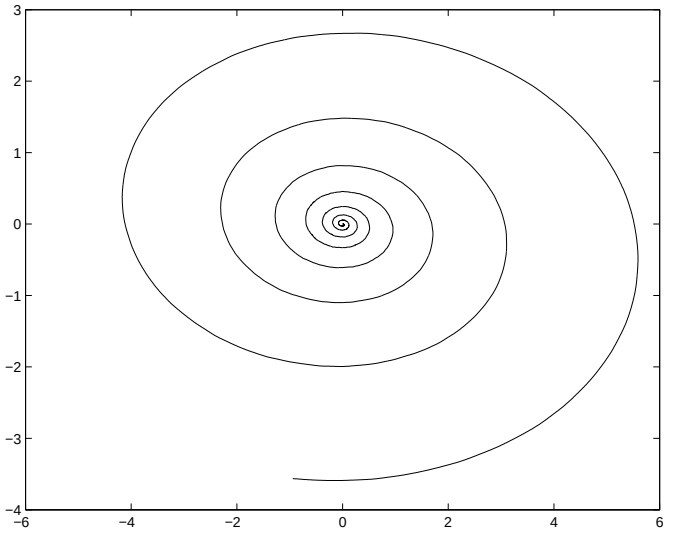

Figure 7: Ψ vs Θ trajectory for super-critical value $\sigma = 1.08$.

In practice elastic structures have linear restoring forces only for displacements of very small magnitude. From a potential energy form $\frac{1}{2}\, X^* \mathbf{A}\, X$ one derives a linear restoring force $-\nabla \left(\frac{1}{2}\, X^* \mathbf{A}\, X\right) =$

$-\mathbf{A}\,X$. Physical realism leads one to assume that the actual restoring force depends in a nonlinear manner on X that can be approximated via a potential energy form

$$\frac{1}{2}\,X^*\mathbf{A}\,X\,+\,\frac{\epsilon}{4}\,(X^*\mathbf{A}\,X)^2$$

from which one obtains a restoring force

$$-\,\nabla\left(\frac{1}{2}\,X^*\mathbf{A}\,X\,+\,\frac{\epsilon}{4}\,(X^*\mathbf{A}\,X)^2\right)\,=\,-\,\mathbf{A}\,X\,-\,\epsilon\,(X^*\mathbf{A}\,X)\,\mathbf{A}\,X.$$

For small values of ϵ this modification of the restoring force can be expected to dominate for moderate to large values of $\|X\|$ and prevent a linearly unstable system from generating unbounded trajectories. In the work reported here this procedure was applied to the elastic beam restoring forces.

Using $\epsilon\,=\,.0001$ and the system whose Θ, Ψ trajectories for $\epsilon\,=\,0$ (linear system) are shown in Figure 7 we obtain the trajectories shown in Figure 8.

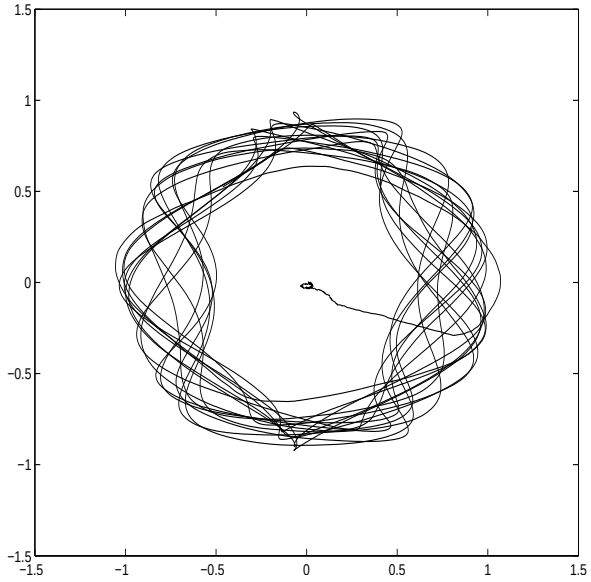

Figure 8: Ψ vs Θ trajectory for super-critical value $\sigma\,=\,1.08$;
nonlinear restoring force added.

This is a classic precession plot, showing that the fan axis motion is composed of two cyclical parts with different frequencies. If we increase to $\sigma\,=\,1.25$ the effect is stronger, as shown in Figure 9. Increasing to $\sigma\,=\,1.4$ we obtain a "crown" pattern as shown in Figure 10, corresponding to a very violent precessional motion. Note in all of these cases the "tail" part of the trajectory, showing

a small initial state moving out to the larger quasi-steady state precessional trajectory.

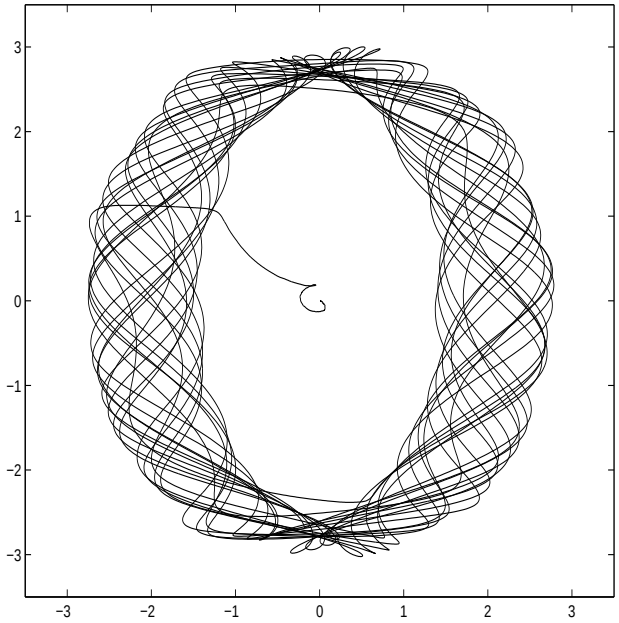

Figure 9 : Ψ vs Θ trajectory for super-critical value $\sigma = 1.25$;
nonlinear restoring force added.

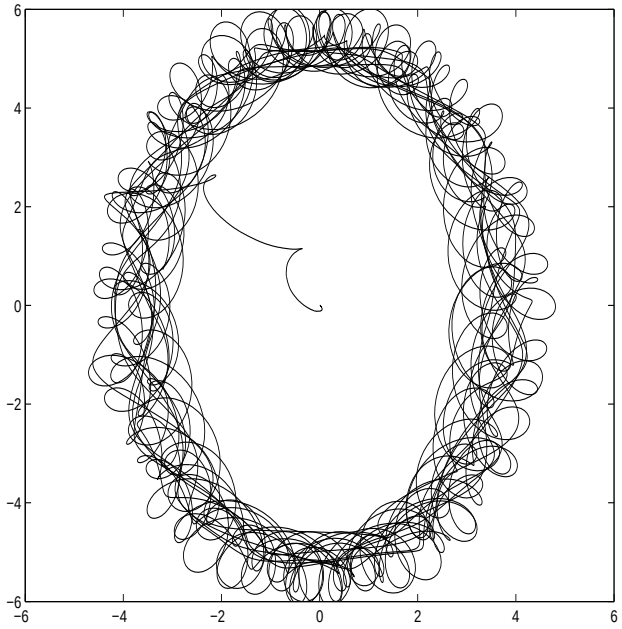

Figure 10 : Ψ vs Θ trajectory for super-critical value $\sigma = 1.4$;
nonlinear restoring force added.

It is clear that the precessional motion associated with larger values of σ and assumed nonlinear restoring forces poses, in an actual physical situation, real dangers to the structural integrity of the wind energy system under study. In order to remedy this situation it is necessary to introduce active controls into the modeled system. Taking the physical circumstances into account it will be clear that it is not feasible to apply such control forces directly from an external source. Thus proof mass actuators are introduce as described in §2. The mode of actuation studied here corresponds to a proof mass actuator acting in the Z direction with its axis passing through the center of mass of the generator head unit. The actuator is applied to the system whose uncontrolled motion is shown in Figure 8, corresponding to $\sigma = 1.08$. The result for a time interval of intermediate length is shown in Figure 11.

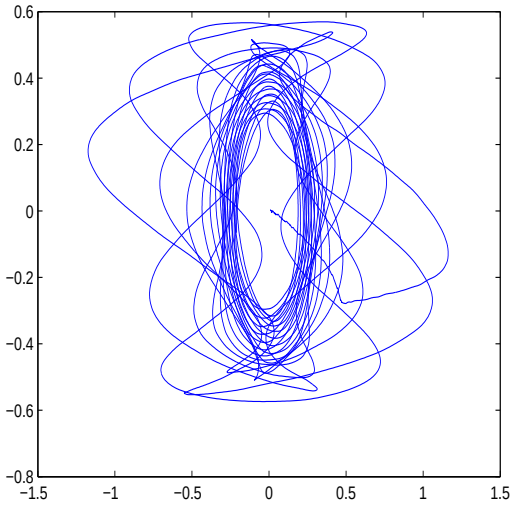

Figure 11 : Ψ vs Θ trajectory for super-critical value $\sigma = 1.08$;
nonlinear restoring force added; proofmass actuator applied.

A related study, extending over a longer interval, is shown in Figure 12. In both of these instances the system enters the nonlinear domain before the actuator takes full effect. Then the nonlinear vibrations are damped out and the system returns to the intermediate linear region and begins slow decay toward the zero equilibrium.

Proof mass actuators need to be carefully tuned, by selection of the relevant parameters described in §2, for optimal damping performance. The procedures currently available for this tuning exercise are generally valid for a single vibrational frequency, or a small number of such frequencies, and are generally developed for a linear structure. In Figure 13 we show $\log|f|$ for f the discrete Fourier transform of the Ψ trajectory corresponding to Figure 12. The upward peaks in this plot are located at abscissae which correspond to frequencies present in the signal. It is clear that there are many of these in this case. Future work connected with our modeled structure thus needs to be directed toward accommodating a large number of vibrational frequen-

cies in a nonlinear context. Relevant mathematical tools remain to be developed for this task.

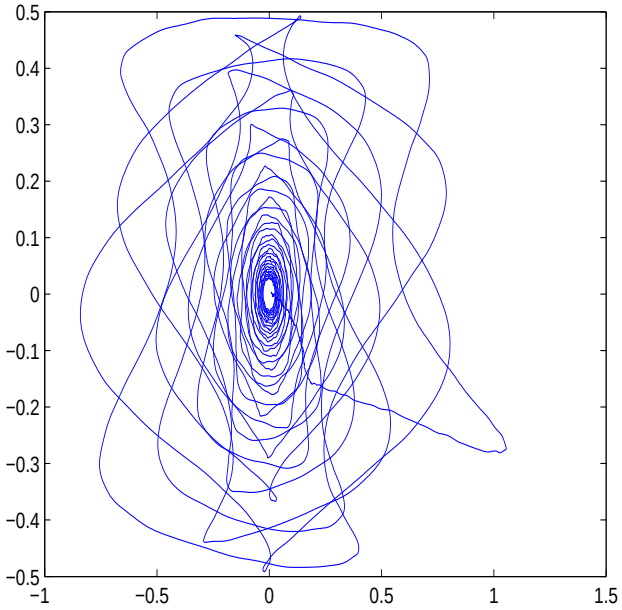

Figure 12: Another Ψ vs Θ trajectory for super-critical value $\sigma = 1.08$; nonlinear restoring force added; proofmass actuator applied.

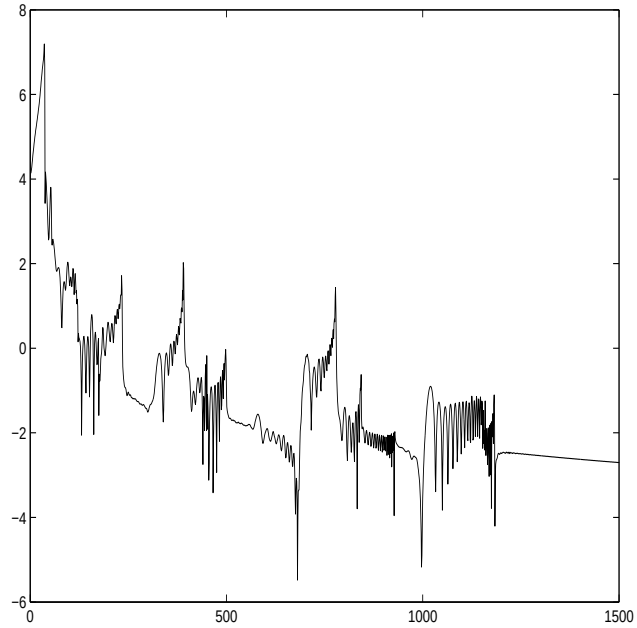

Figure 13: $\log|f|$, f the discrete Fourier transform of $\Psi(t)$ as in Figure 12.

6 Concluding Remarks

The major contribution of this study is the design of a model of a controlled wind turbine as a distributed parameter system using classical mechanics. We have allowed for both lateral and torsional motion in the supporting pylon and the generator unit was modeled as a lumped (finite dimensional) system coupled to the free end of the beam. We computed the potential and kinetic energy integrals of the beam and the fan using classical mechanics and added them to obtain the total energy integrals of the system while translating the fan energy integrals into the coordinate system of the beam. Then to develop a model of the combined structural and rotational motion of the fan coupled with the supporting pylon we used Hamiltonian principles and developed a hybrid system of ordinary and partial differential equations.

The use of proof mass actuators at the top of the generator head is proposed to function as an external vibration control mechanism. We have noted that the requisite tuning of proof mass actuators in order to suppress multi-frequency vibrations is a process not fully developed at the present time. The need for additional studies in this area is clearly indicated.

Instead of solving the coupled PDE/ODE system to obtain a closed form solution - an unrealistic goal in view of the high dimensionality involved - a numerical method was developed using cubic B-splines for the continuous supporting pylon structure. The model was realized by using cubic spline approximation, translating the continuous physical model to a discrete system. We used MATLAB$^{(R)}$ for our simulations. With extensive experimentation based on $n = 4$ spline subintervals we verified that discretization provided sufficient structural flexibility for analysis of the pylon without encountering serious problems of inaccuracy or ill-conditioning. Our work demonstrates that the model is well represented by using cubic B-Splines and compares favorably to established conclusions of related physical experiments.

The simulations undertaken and the resulting vibration diagrams that we have included show that precession type vibrational instabilities result at high fan rotation rates when nonlinear restoring forces are included in the model and that proof mass actuators show promise for mitigating the effects of such instabilities, especially if appropriated tuning methods can be developed.

References

[1] Donnell, L. H., *Beams, Plates and Shells*, McGraw - Hill Pub. Co., New York, 1976.

[2] D., Barry, and E. Garcia: *Optimal placement of a proof mass actuator for active structural acoustic control*, Mech. Struct. Mach., **27** (1996), no. 1, pp. 23-35.

[3] Laurence V. Fausett: *Applied Numerical Analysis Using Matlab*, Pentice Hall, Upper Saddle River, NJ, 1999.

[4] Gantmacher, F. R.: *Theory of Matrices*, Vols. I, II, AMS Chelsea Pub. Ser., 1990.

[5] Goldstein, H.:*Classical Mechanics*, Addison-Wesley,1950.

[6] Huyanan, S., and N. D. Sims: *Vibration control strategies for proof-mass actuators*, J. Vib. & Control, **13** (2007), no. 12, pp. 1785-1806.

[7] Keane, M. K.: *A Very Applied First Course in Partial Differential Equations*, Prentice-Hall, Inc., Upper Saddle River, NJ, 2002.

[8] Kincaid, D., and W. Cheney: *Numerical Analysis : Mathematics of Scientific Computing*, 3rd ed., Brooks/Cole Pub. Co., Pacific Grove, CA, 2002.

[9] Lagnese, J., and G. Leugering: *Uniform energy decay of a class of cantilevered nonlinear beams with nonlinear dissipation at the free end*, in Differential Equations with Applications in Biology, Physics, and Engineering (Leibnitz,1989), pp. 227-239, Lec. Notes pure and Appl. Math., 133, Marcel Dekker, NY, 1991.

[10] Manwell, J. F., J. G. McGowan and A. L. Rogers: *Wind Energy Explained: Theory, Design and Application*, 2nd ed., John Wiley & Sons, New York, 2010.

[11] Politansky, H., and W. D. Pilkey: *Suboptimal feedback vibration control of a beam with a proof-mass actuator*, J. Guid. & Contr. Dyn., **12** (1989), no. 5, pp. 691-697.

[12] Quinn, J.P., and David L. Russell: *Assymptotic stability and energy decay rates for solutions of hyperbolic equations with boundary damping*, Proc. Roy. Soc. Edinb., Sect. A, **77A** (1977), no. 1-2, pp. 97-127.

[13] David L. Russell: *On boundary-value controllability of linear symmetric hyperbolic systems*, 1967 Mathematical Theory of Control (Proc. Conf., Los Angeles, CA), pp.312-321, Academic press, NY, 1967.

[14] David L. Russell: *http://www.math.vt.edu/people/dlr/ma4446nt.html*, Class Notes, 2011.

[15] Symon, Keith R.: *Mechanics*, 2nd ed. Addison-Wesley Series in Physics, Addison-Wesley Publishing Co., Inc., Reading, Mass., London, 1960.